Supplementary Information for

Effects of biological buffer solutions on the peroxidase-like catalytic activity of Fe_3O_4 nanoparticles

Mariana Raineri[a], Elin L. Winkler[a,b], Teobaldo E. Torres[a], Marcelo Vasquez Mansilla[a], Marcela S. Nadal[c], Roberto D. Zysler[a,b], Enio Lima Jr.*[a]

[a.] *Instituto de Nanociencia y Nanotecnología - Nodo Bariloche, CNEA, CONICET, Centro Atómico Bariloche, Av. Bustillo 9500 (8400) S. C. Bariloche, Argentina.*
[b.] *Instituto Balseiro CNEA-Universidad Nacional de Cuyo, Centro Atómico Bariloche, Av. Bustillo 9500, 8400, San Carlos de Bariloche, Argentina.*
[c.] *Dep. Física Médica, CNEA, Centro Atómico Bariloche, Av. Bustillo 9500 (8400) S. C. Bariloche, Argentina.*

** lima@cab.cnea.gov.ar*

Supplementary Information - Supplementary Results & Discussion

Nanoparticle Characterization. IONPs were morphologically characterized by Transmission Electron Microscopy (TEM) as shown in Supplementary fig. S1A. For the synthesized IONPs, the particle size histogram shows a lognormal distribution centered at the mean value <d> = 21.00 nm with standard deviation of σ = 0.34 (fig. S1B). As expected, the particles exhibit hydrophobic character due to the coating with a layer of oleic acid added once the synthesis is completed. The presence of oleic acid is demonstrated by two absorption peaks at 2921 cm^{-1} and 2853 cm^{-1} that can be attributed to the asymmetric CH_2 and the symmetric CH_2 stretching, respectively (figure S1C, black line). At the same time, the binding of the oleic acid to the iron in the particles is demonstrated by the presence of COO^- (peaks at 1565 cm^{-1} and 1399 cm^{-1}) and the absence of the characteristic C=O stretch vibration of the unbound COOH group at 1700-1725 cm^{-1} present in the free oleic acid spectra, indicating that oleic acid is chemisorbed onto the nanoparticles as a carboxylate[1]. Oleic acid must be removed in order for IONPs to be dispersed in water and all the aqueous buffer solutions. After repeated washing of the IONPs (figure S1C, blue line), in the normalized absorption spectra to the peak of Fe-O at 555 cm^{-1}, the disappearance of the characteristic peaks of oleic acid indicates that the particles are naked, and hence, the superficial iron is readily available to participate in peroxidation reactions. In Supplementary Figure S2, the XRD pattern of the IONPs is presented in order to confirm the presence of the ferrite structure expected for the Fe_3O_4 magnetite. The Fe^{2+} content in the IONPs before (oleic acid coated) and after the washing procedure (naked particles) were determined by XPS, as shown in Supplementary figure S3.

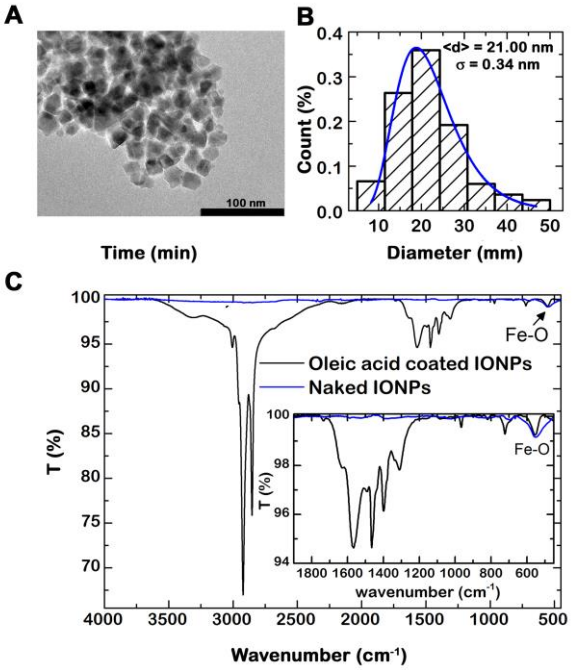

Supplementary figure S1. TEM and FTIR results of the as-prepared nanoparticles. (A) Representative TEM image of the IONPs showing the morphology of the particles and, (B) the corresponding particle-size distribution. (C) FTIR spectra of IONPs before and after being washed. Note the absence of oleic acid characteristic peaks in the washed particles.

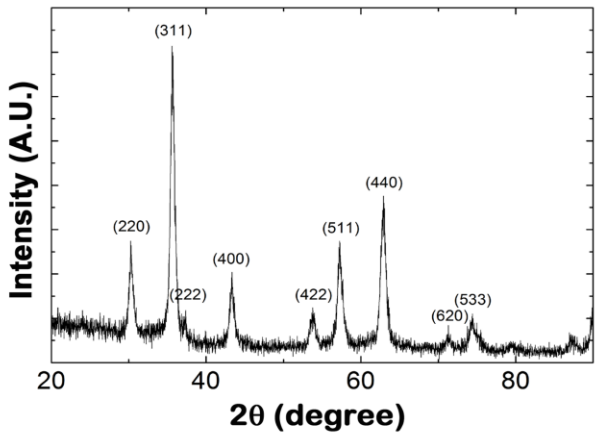

Supplementary figure S2. XRD pattern of the as-prepared IONPs coated with oleic acid. The peaks were indexed with the corresponding crystallographic planes of magnetite (JCPDS card N° 19-0629).

According to the XPS spectra, the Fe^{2+}/Fe ratio was 0.25 for the as-made IONPs, 0.23 after washing the as-made IONPs and 0.17 for the naked IONPs stored in water for 1 year. Despite the fact that the expected Fe^{2+}/Fe ratio was not exactly the one of the magnetite (0.33), before and after washing the IONPs this ratio remained almost unchanged, indicating that little oxidation of Fe^{2+} occurred. Moreover, during the storage in water for almost 1 year at 4ºC, the Fe^{2+} content decreased to 17 %, meaning that the oxidation process is relative slow and therefore we expected to remain invariant over the temporal window in which we performed all of the experiments.

As shown in Supplementary Scheme S4A (adapted from Frey *et al.*[2]), the non-oxidized TMB has an absorption peak at λ_{max} = 265 nm. The oxidation of TMB catalyzed by the peroxidase enzyme in solution proceeds via two-electron oxidizing steps that begins with the formation of a blue intermediate (λ_{max} = 370 nm and 652 nm), which is further oxidized to a yellow final product with an absorption peak at λ_{max} = 450 nm[2,3]. Although there are two product species in equilibrium that absorb at different wavelengths, the reaction is evaluated by recording the

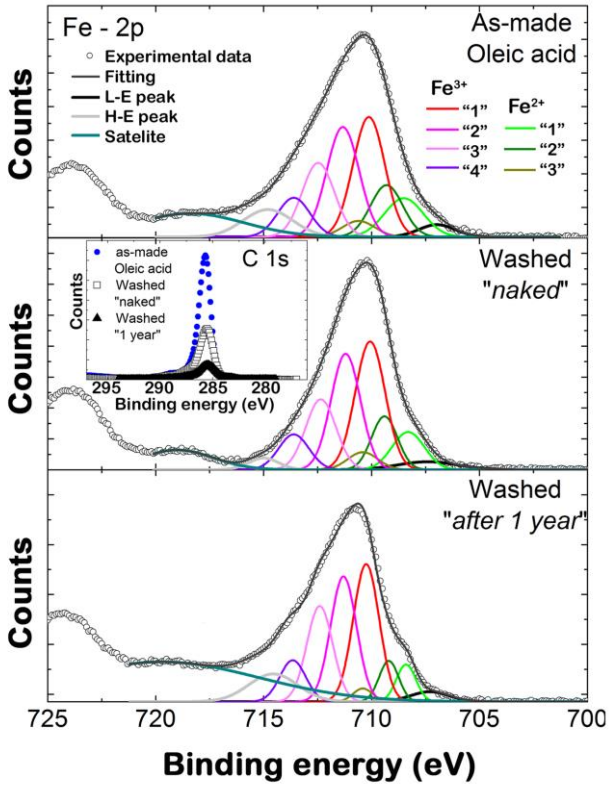

Supplementary figure S3. XPS spectra in the Fe-2p binding energy range of the as-made IONPs coated with oleic acid before the washing procedure (upper panel), after being washed (middle panel) and the naked IONPs one year kept in water in the fridge. All the spectra were fitted considering a Shirley background. The $2p_{3/2}$envelope is fitted taking the multiplets related to the contribution of the Fe^{2+}, Fe^{3+}, satellites, high-energy peak of surface structure and a pre-peak.

Sample	Contribution	peak	E (eV)	w	A	A%	E_{ref}	$A\%_{ref}$	Total Area	ΔE (%)	ΔA (%)	Fe^{2+}/Fe	Formula
As-made	LE-BE	1	707.0	1.7	780	-	706.3	-	-	0.10	-	0.25	$Fe^{2+}_{0.75}Fe^{3+}_{2.25}O_4$
	Fe^{2+}	1	708.5	1.8	2600	40.63	708.3	41.6	6400	0.03	2.34		
		2	709.3	1.5	2900	45.31	709.3	43.2		0.00	-4.89		
		3	710.6	1.5	900	14.06	710.4	15.2		0.03	7.48		
	Fe^{3+}	1	710.2	1.5	6599	34.56	710.3	34.9	19093	-0.01	0.97		
		2	711.3	1.5	6151	32.22	711.1	31.8		0.03	-1.31		
		3	712.5	1.5	4147	21.72	712.3	22.6		0.03	3.89		
		4	713.6	1.5	2196	11.50	713.6	10.8		0.00	-6.50		
	HE-BE	1	714.8	2.3	2349	-	714.3	-	-	0.07	-		
	Satellite	1	718.4	5	4379	-	718.6	-	-	-0.03	-		

Supplementary Table 1. Data extracted from the XPS experiment. E is the Binding Energy of the peak center, w is the peak width, A is the area of each peak, A% is the percentage contribution of each peak for the total area of the respective Fe ion, E_{ref} and A_{ref} reference values of E and A obtained from literature[4].

Sample	Contribution	peak	E (eV)	w	A	A%	E_{ref}	$A\%_{ref}$	Total Area	ΔE (%)	ΔA (%)	Fe^{2+}/Fe	Formula
Naked IONP (washed)	LE-BE	1	707.4	2.78	900	-	706.3	-	-	0.16	-	0.23	$Fe^{2+}_{0.69}Fe^{3+}_{2.31}O_4$
	Fe^{2+}	1	708.3	1.5	2300	38.98	708.3	41.6	5900	0.00	6.29		
		2	709.4	1.2	2600	44.07	709.3	43.2		0.01	-2.01		
		3	710.4	1.5	1000	16.95	710.4	15.2		0.00	-11.51		
	Fe^{3+}	1	710.1	1.43	7200	36.74	710.3	34.9	19599	-0.03	-5.26		
		2	711.2	1.45	6387	32.59	711.1	31.8		0.01	-2.48		
		3	712.4	1.4	4000	20.41	712.3	22.6		0.01	9.69		
		4	713.6	1.4	2012	10.27	713.6	10.8		0.00	4.95		
	HE-BE	1	715.0	1.4	667	-	714.3	-	-	0.10	-		
	Satellite	1	719.0	3.4	2693	-	718.6	-	-	0.06	-		
Naked IONP (1 year after the washing procedure)	LE-BE	1	707.4	1.8	688	-	706.3	-	-	0.16	-	0.17	$Fe^{2+}_{0.51}Fe^{3+}_{2.49}O_4$
	Fe^{2+}	1	708.5	1.4	2000	41.24	708.3	41.6	4850	0.03	0.87		
		2	709.4	1.4	2150	44.33	709.3	43.2		0.01	-2.62		
		3	710.4	1.4	700	14.43	710.4	15.2		0.00	5.05		
	Fe^{3+}	1	710.4	1.6	7955	33.22	710.3	34.9	23945	0.01	4.81		
		2	711.2	1.6	7795	32.55	711.1	31.8		0.01	-2.37		
		3	712.4	1.6	5595	23.37	712.3	22.6		0.01	-3.39		
		4	713.6	1.6	2600	10.86	713.6	10.8		0.00	-0.54		
	HE-BE	1	714.8	2.3	2998	-	714.3	-	-	0.07	-		
	Satellite	1	720.0	9	18062	-	718.6	-	-	0.19	-		

Supplementary Table 2 (cont). Data extracted from the XPS experiment. E is the Binding energy of the peak center, w is the peak width, A is the area of each peak, A% is the percentage contribution of each peak for the total area of the respective Fe ion, E_{ref} and A_{ref} reference values of E and A obtained from literature[4].

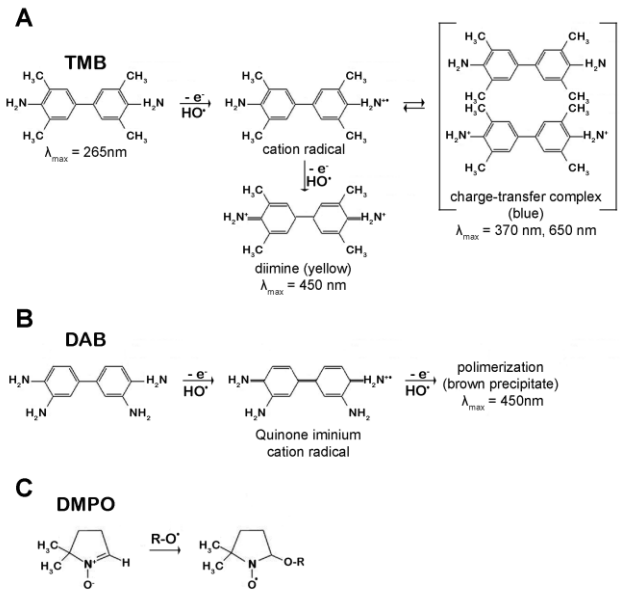

Supplementary Scheme S4. Oxidation reactions of the peroxidase substrates and the spin-trap DMPO. (A) Oxidation mechanism and color development of TMB and (B) DAB substrates. (C) DMPO reaction mechanism to form a DMPO-adduct radical (R) that can be measured by EPR.

absorbance of only the blue intermediate at 650 nm. For this reason, DAB oxidation was also included in order to validate the results. The polymerized form of DAB, which is the highest oxidation species formed during the reaction, is evidenced by the presence of only one peak at λ_{max} = 450 nm (Supplementary Material S4B, adapted from Nateghi *et al.*[5]). Schematic DMPO reaction with radical species is shown in the Scheme S4C.

We aimed to study the stability of H_2O_2 by using ATR-FTIR to monitor the decay of the O-H peak (2835 cm^{-1})[6]. Absorbance spectra of H_2O_2 in acetate buffer recorded at different times are shown in Supplementary Information S5A and the inset shows in detail the 2835 cm^{-1} peak region. Acetate buffer spectrum was subtracted from each H_2O_2 spectra (Supplementary Information S5B), and the height of the 2835 cm^{-1} peak was used to monitor H_2O_2 decay. Decomposition of H_2O_2 displayed a linear response when plotting $1/[H_2O_2]$ against the reaction time, following a second order-reaction kinetic[7], as shown in Supplementary Information S5C. In the presence of IONPs, decomposition of H_2O_2 is accelerated due to their catalytic activity.

As revealed in Supplementary Information S5D, H_2O_2 stability was similar in solutions of phosphate of different molarity but in the presence of IONPs, the decay was accelerated as phosphate concentration decreased in pH 5.0, in agreement with the higher catalytic activity observed for PB 0,001 M. We also observed higher H_2O_2 stability at pH 5.0 *vs* pH 7.4 (slope = 1.50 *vs*

1.75/M·min, respectively) as shown in Supplementary Information S5E, but when IONPs were included in the reaction, similar decomposition rates are observed for pH = 5.0 (slope = 2.18/M·min) and pH = 7.4 (slope = 2.14/M·min). This could mean that although decomposition rates of peroxide are similar in both pH solutions, in physiological pH solutions other reactions that are different from peroxidase-like reactions but which also consume H_2O_2, yet produce less free radical species, might be happening. One possible explanation is that catalase-like activity of IONPs is privileged at this pH and would lead to H_2O_2 decomposition into H_2O and O_2[8]. Since salinity itself could be altering the peak shape of H_2O_2 spectra[9], no comparisons were made between PB and PBS. Furthermore, H_2O_2 stability in HEPES was remarkably accelerated with IONPs, yet there seems to be little difference after bicarbonate addition except for a slight increase of H_2O_2 decomposition in the HEPES-bicarbonate combination with IONP (Supplementary Information S5F).

Supplementary Information S6
Supplementary Methods

Chemicals. Drugs were purchased either from Anedra (Hydrogen peroxide); Biopack (Sodium Acetate); Cicarelli (Sodium Bicarbonate); Mallinckrodt Pharmaceuticals Inc. (Disodium hydrogen phosphate; Potassium dihydrogen Phosphate; Sodium Chloride and Sodium Carbonate); Merck Millipore (Acetic Acid) or Sigma-Aldrich (DMPO >97 %; DMSO >99 %; DAB; HEPES). TMB ready to use solution was obtained from Ingenasa (Madrid, Spain). The chemical reagents used in the synthesis of the nanoparticles were Oleic acid (analytical standard), Oleylamine (70 %), benzyl ether (98 %), 1,2-octanediol (98 %) and Fe(III) acetylacetonate (97 %). Methanol and Ethanol were technical grade, acetone (reag. Ph Eur.), chloroform (> 99 %), toluene (99.8 %) and hydrochloric acid (HCl – 37 %). Quartz tubes of 2 mm of thickness were used in the EPR experiments. MgO crystal doped with Mn^{2+} ions was prepared by specialized co-workers.

Nanoparticle Preparation. Briefly, 3 mM of Fe(III) acetylacetonate ($Fe(acac)_3$), 9 mM of oleic acid, 9 mM of oleylamine and 1.5 mM of 1,2-octanediol were mixture in 60 mL of benzyl ether in a tree-neck-flask with mechanical stirring. The system was heated up with N_2 flux (0.5 L/min., 5.0) up to 110-130 °C during 30 minutes for humidity removal and heated to the reflux at 295°C condition during 60 minutes. Finally, the system was rapidly cooled down to room temperature. IONP were precipitated by addition of 400 mL of ethanol and 40 mL of acetone and magnetically separated with a permanent magnet. IONP were suspended in toluene and then washed with a mixture of ethanol and acetone. In order to remove the oleic acid present in the as-prepared nanoparticles, they were washed with methanol for 8 h, followed by 46 h incubation in acetone at 40 °C. Naked particles were obtained after adding 10 mL of toluene followed by removal of the supernatant. Only the precipitated nanoparticles were collected.

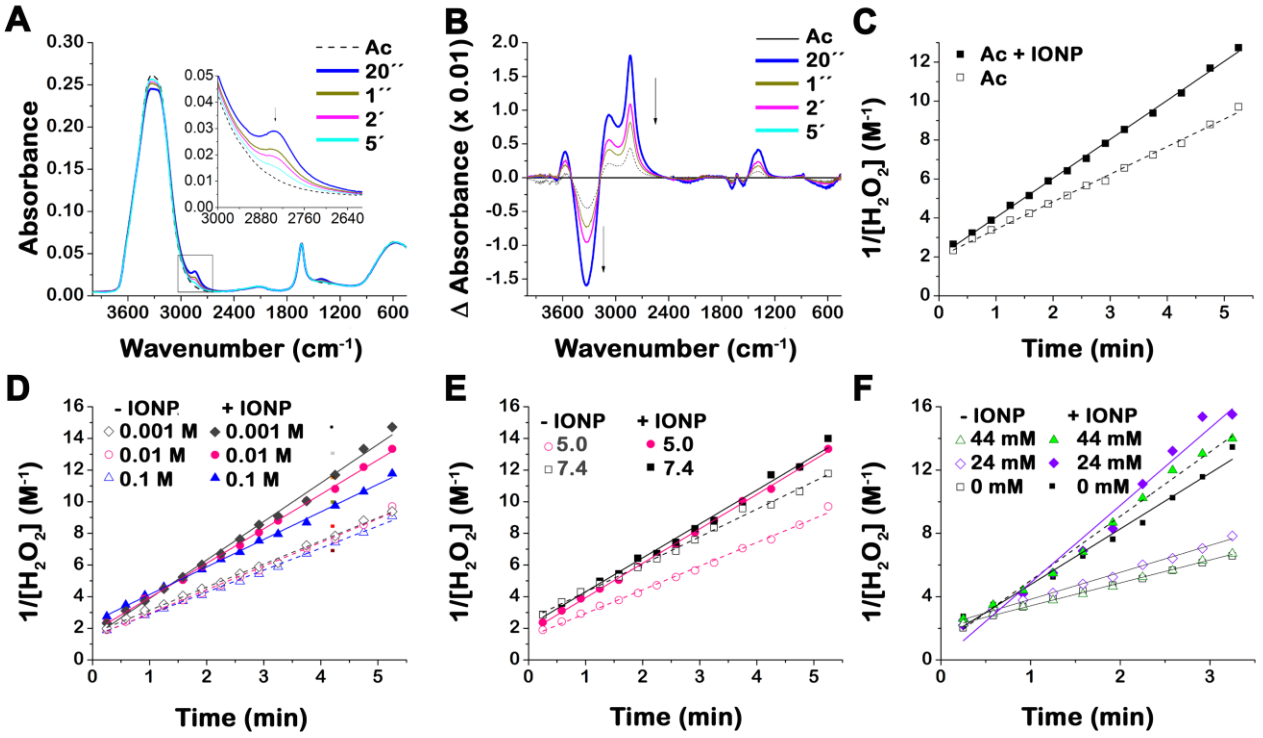

Supplementary figure S5. ATR-FTIR measurement of IONPs-catalyzed decomposition of H_2O_2. (A) ATR-FTIR sequential absorbance spectra of H_2O_2 in buffer and the detailed 2600-3000 cm^{-1} range where the disappearance of the 2835 cm^{-1} peak occur (inset). (B) H_2O_2 absorbance spectra normalized to acetate buffer spectrum. (C) IONP catalyzed decomposition rate of H_2O_2 in acetate. H_2O_2 decomposition rate in: (D) phosphate buffer of different concentrations (0.1 – 0.001 M), (E) Phosphate buffer of different pH (5.0-7.4) and, (F) HEPES-bicarbonate buffer.

Nanoparticle Characterization. Transmission Electron Microscopy (TEM) images were obtained in a Tecnai F20-G2 (Thermo Fisher Scientific, formerly FEI) microscope operating at 200 kV at room temperature. TEM specimens were prepared by dispersing the dried powder of nanoparticles in chloroform and dropping the solution onto a carbon covered copper grid. The mean particle size (<d>) and the size dispersion (σ) were determined by measuring the diameter of more than 500 particles and fitting the corresponding histogram with a log-normal distribution.

X-ray diffraction pattern was taken in a Philips PW 346 diffractometer by using the CuKα radiation (λ=0.154186 nm) at room temperature in a sample conditioned over a glass surface. Magnetite JCPDS card N° 19-0629 was used as the reference to identify the peak corresponding to each crystallographic plane, being this phase the unique contribution observed.

Oxidation state of iron in the IONP sample was obtained by X-ray photoelectron spectroscopy measurements in the Fe-$2p_{3/2}$ binding energy range[10]. Measurements were performed in a SPECS spectrometer using a 150 mm Phoibos hemispherical analyzer in the energy range of Al-Kα (1486.6 eV) and a chamber pressure of 10^{-10} mBar. The fitting procedure used for each sample was similar to that reported in Grosvenor *et al*[4]. A Shirley-type background was used in order to remove most of the extrinsic loss structure. The Fe-$2p_{3/2}$ envelope was fitted using multiplets (3 peaks corresponding to the Fe^{2+} and 4 peaks for the Fe^{3+} in the ferrite structure) with correlations among the binding energy and the peak areas. High-energy peaks corresponding to the surface of the structures and shake-up-related satellites were also added. The binding energy for each sample was calibrated using the C1s peak position with the reference value of 284.8 eV.

Catalytic activity determined by the TMB oxidation. Catalytic activity using the TMB oxidation was determined incubating 80 µg of IONP (dispersed in 100 µl of ultrapure water) with 700 µl of the buffer solution in a 1 ml cuvette. After equilibration with 100 µl of TMB commercial substrate solution, 100 µl of H_2O_2 (30%) was added to start the reaction. Absorbance (650 nm) was recorded every 10 seconds for a total of 300 seconds with an UV-VIS Spectrophotometer 1800 (Shimadzu Scientific Instruments). Activity units were calculated as µmol of oxidized TMB ($\epsilon_{562\ nm}$ = 39,000 M^{-1} cm^{-1}) produced per minute[11]. All the catalytic experiments were conducted at room temperature (20 ± 2°C). To investigate free iron effect on IONP catalytic oxidation of TMB, $FeSO_4.7H_2O$ and $FeCl_3.6H_2O$ were dissolved in the buffer at the same concentration of Fe_3O_4 determined in our IONP by the thiocyanate method. Absorbances were measured in arbitrary units. Catalytic oxidation determined by the DAB oxidation was determined incubating 25 µg of IONPs (suspended in 30 µl of ultrapure water) with 720 µl of buffer in a 1 ml cuvette. Then, 30 µl of DAB (10 mg/ml) was added and after 1 min stabilization of the mixture, 30 µl of H_2O_2 (30%) were incorporated to start the reaction. Absorbance (450 nm) was recorded every 10 seconds for a total of 300 seconds with an UV-VIS Spectrophotometer 1800 (Shimadzu Scientific Instruments). For microplate reaction measurements, concentrations were adapted to a final volume of 300 µl and absorbance was recorded in a 96-well microplate (Greiner Bio One) with a microplate reader (Thermo Scientific™ Multiskan™ GO Microplate Spectrophotometer) for a total period of time of ~ 60 min. All measurements were performed at 20 ± 3 ºC.

Attenuated Total Reflectance Spectroscopy. FTIR measurements were performed in a Spectra Two spectrometer (Perkin Elmer) using the uATR optical configuration using diamond as ATR material. A total of 4 scans were averaged for each spectrum at a spectral resolution of 4 cm^{-1}. For desorption studies of buffer species from IONP surface, we used the nanoparticle film approach. Briefly, IONP were incubated in the buffer solution for 24 h. Then, by using a magnet to recover the particles, two washes in ultrapure water were performed. Measurements were performed by dropping 10 µL of the solution containing the nanoparticles onto the uATR-diamond. IONP were dried with N_2 flux and collected spectra were processed for the baseline subtraction and ATR correction with the software Spectrum 10 (Perkin Elmer). Once the film was constituted, a sample holder was placed above the film. 30 µl of buffer was placed in the holder and an initial spectrum was recorded. After H_2O_2 addition (0.44 mM), spectra was recorded every 60 seconds (4 scans) for 5 min. Initial spectrum (without H_2O_2) was subtracted to every spectra and the area of a characteristic peak of each of the buffer species were integrated. Namely, 1077 cm^{-1} peak for acetate, 986-1030 cm^{-1} band region for PB, 770 cm^{-1} peak for HEPES and the 1250-1050 cm^{-1} absorption region for bicarbonate. For the ATR-FTIR measurements of H_2O_2 decomposition we used a sample holder accessory (Perkin-Elmer). Initial scan was performed incubating 20 µg of IONP and 31 µl of the buffer solution. After H_2O_2 addition (0.44 mM), spectra was recorded every 20 seconds (2 scans), and each sequence lasted 15 sec, for 5 min. Initial spectrum (without H_2O_2) was subtracted to every spectra and the O–H stretching vibration (2930–2680 cm^{-1})[9] band height were converted into H_2O_2 concentration values by constructing a standard curve. Then, $1/[H_2O_2]$was plotted against time after fitting various kinetic order equations.

Supplementary bibliography

1 L. Zhang, R. He and H. C. Gu, *Appl. Surf. Sci.*, 2006, **253**, 2611-17.

2 A. Frey, B. Meckelein, D. Externest and M. A. Schmidt, *J. Immunol. Methods*, 2000, **233**, 47–56.

3 P. D. Josephy, *Environ. Health Perspect.*, 1985, **64**, 171–178.

4 A. P. Grosvenor, B. A. Kobe, M. C. Biesinger and N. S. McIntyre, *Surf. Interface Anal.*, 2004, **36**, 1564–1574.

5 M. R. Nateghi, M. H. Mosslemin and H. Hadjimohammadi, *React. Funct. Polym.*, 2005, **64**, 103–109.

6 E. Erasmus, J. Claassen and W. Van der Westhuizen, *Water SA*, 2016, **42**, 442.

7 S. M. Badawy, R. A. El Khashab and A. A. Nayl, *Bull. Chem. React. Eng. Catal.*, 2015, **10**, 169–174.

8 Z. Chen, J.-J. Yin, Y.-T. Zhou, Y. Zhang, L. Song, M. Song, S. Hu and N. Gu, *ACS Nano*, 2012, **6**, 4001–4012.

9 H. Voraberger, V. Ribitsch, M. Janotta and B. Mizaikoff, *Appl. Spectrosc.*, 2003, **57**, 574–579.

10 K. Mishra, T. N. Poudel, N. Basavegowda and Y. R. Lee, *J. Catal.*, 2016, **344**, 273–285.

11 B. Jiang, D. Duan, L. Gao, M. Zhou, K. Fan, Y. Tang, J. Xi, Y. Bi, Z. Tong, G. F. Gao, N. Xie, A. Tang, G. Nie, M. Liang and X. Yan, *Nat. Protoc.*, 2018, **13**, 1506–1520.